

## Sonic anemometry measurements to determine airflow patterns in multi-tunnel greenhouse

A. López, D. L. Valera\*, F. D. Molina-Aiz and A. Peña

*Universidad de Almería. Campus de Excelencia Internacional Agroalimentario ceiA3.  
Ctra. de Sacramento s/n. 04120 Almería, Spain*

---

### Abstract

The present work describes a methodology for studying natural ventilation in Mediterranean greenhouses using sonic anemometry. The experimental work took place in the three-span greenhouse located at the agricultural research farm belonging to the University of Almería. This methodology has allowed us to obtain patterns of natural ventilation of the experimental greenhouse under the most common wind regimes for this region. It has also enabled us to describe how the wind and thermal effects interact in the natural ventilation of the greenhouse, as well as to detect deficiencies in the ventilation of the greenhouse, caused by the barrier effect of the adjacent greenhouse (imply a mean reduction in air velocity close to the greenhouse when facing windward of 98% for  $u$ , 63% for  $u_y$ , and more importantly 88% for  $u_x$ , the component of air velocity that is perpendicular to the side vent). Their knowledge allows us to improve the current control algorithms that manage the movement of the vents. In this work we make a series of proposals that could substantially improve the natural ventilation of the experimental greenhouse. For instance, install vents equipped with ailerons which guide the air inside, or with vents in which the screen is not placed directly over the side surface of the greenhouse. A different proposal is to prolong the opening of the side vents down to the soil, thus fomenting the entrance of air at crop level.

**Additional key words:** buoyancy; insect-proof screens; natural ventilation; wind effect.

### Resumen

#### Determinación de los patrones de flujo de aire en un invernadero multitúnel mediante anemometría sónica

En este trabajo se ha desarrollado una metodología para estudiar la ventilación natural en invernaderos mediterráneos mediante anemometría sónica. Los ensayos se han realizado en un invernadero multitúnel de tres módulos situado en el Campo de Prácticas de la Universidad de Almería. Esta metodología nos ha permitido obtener los patrones de ventilación natural del invernadero experimental para los vientos más comunes de la región. También nos ha permitido describir la interacción entre el efecto eólico y térmico, así como detectar deficiencias en la ventilación natural del invernadero debidas al efecto barrera de otro invernadero adyacente (provocando una reducción media en la velocidad del aire en el exterior de la ventana de barlovento de hasta el 98% para  $u$ , 63% para  $u_y$  y, más importante, 88% para  $u_x$ , la componente de la velocidad del aire que es perpendicular a la superficie de ventilación lateral). Los conocimientos adquiridos en este trabajo nos permitirán mejorar los algoritmos de control del sistema de ventilación. En este trabajo se realizan una serie de propuestas que podrían mejorar sustancialmente la ventilación natural del invernadero. Por ejemplo, se proponen algunas posibles modificaciones de la configuración de las ventanas laterales, buscando una mayor captación del aire exterior: se podría optar por ventanas dotadas de alerones exteriores que dirijan al aire hacia el interior o ventanas en las que la malla no se coloque directamente sobre la superficie lateral del invernadero, diseñando una antesala donde el aire pueda entrar sin la oposición de la malla. Otra propuesta sería prolongar la apertura de las ventanas laterales hasta el suelo, para favorecer así la entrada de aire a nivel del cultivo.

**Palabras clave adicionales:** efecto eólico; flotabilidad; mallas anti-insectos; ventilación natural.

---

\*Corresponding author: [dvalera@ual.es](mailto:dvalera@ual.es)

Received: 14-12-11. Accepted: 07-06-12

This work has 1 Supplementary Table and 3 Supplementary Figures that do not appear in the printed article but that accompany the paper online.

## Introduction

Natural ventilation is probably the most common-place method of greenhouse climate control (Boulard *et al.*, 1996; Kittas *et al.*, 1996), and this is particularly true of areas such as the Mediterranean where the implementation of technology in greenhouses has been scant. With a view to optimising the design and handling of natural ventilation systems one must understand both quantitatively (Kittas *et al.*, 1997) and qualitatively how this type of ventilation functions in greenhouses. The main driving forces of ventilation for a greenhouse equipped with both roof and side openings are the result of a combination of pressure differences induced by the following effects (Boulard & Baille, 1995; Kittas *et al.*, 1997): the static wind effect due to the mean component of the wind velocity, which induces pressure differences (side wall effect) between the side and the roof openings (Bruce, 1978) and pressure differences between the windward and the leeward parts of the greenhouse (Boulard *et al.*, 1996); the buoyancy forces (also called stack or chimney effect) generating a vertical distribution of pressures between the side and roof openings (Bruce, 1982); and the turbulent effect of the wind, generated by pressure fluctuations of the wind velocity along and across the greenhouse openings (Boulard & Baille, 1995; Boulard *et al.*, 1996).

Natural ventilation in greenhouses is the result of combining the airflows generated by the wind effect and by the buoyancy of the air (thermal or chimney effect). We can combine these fluxes obtaining different models derived from Bernoulli's equation (Boulard & Baille, 1995; Boulard *et al.*, 1997; Kittas *et al.*, 1997) which allow us to estimate the ventilation rate. Application of these semi-empirical models requires using two fundamental parameters: the pressure drop coefficient through the vent (total discharge coefficient of the opening  $C_d$ ) and the wind effect coefficient (wind effect coefficient for the mean airflow  $C_w$ ), which includes both the stationary and the turbulent aspects of the wind's action. These coefficients are obtained by means of experiments which determine the ventilation rate.

Although many authors have obtained the coefficients  $C_d$  and  $C_w$  that allow the semi-empirical models to be applied (Kittas *et al.*, 1996, 1997; Papadakis *et al.*, 1996; Boulard *et al.*, 1997; Fatnassi *et al.*, 2002; Teitel *et al.*, 2008; Molina-Aiz *et al.*, 2009, 2011), there is still considerable debate as to the exact relationship between the wind and thermal effects in the natural ventilation of greenhouses. Papadakis *et al.* (1996) found that the thermal effect was fundamental for winds of less than  $1.8 \text{ m s}^{-1}$ , while Boulard & Baille (1995) set this speed at  $1.5 \text{ m s}^{-1}$  and Sase *et al.* (1984) at  $1 \text{ m s}^{-1}$ . Other researchers have suggested that in greenhouses equipped with roof vents the thermal effect can be neglected for wind speeds of over  $2 \text{ m s}^{-1}$  (Boulard & Baille, 1995), and this was also suggested for a greenhouse with side and roof vents (Fatnassi *et al.*, 2002). For the latter type of greenhouse, Kittas *et al.* (1997) found that the thermal effect is important when the ratio  $u_o/\Delta T_{io}^{0.5}$  is less than 1, while Bot (1983) set the limit at 0.3.

The earliest studies on the circulation of air in greenhouses date back to the mid-20th century (Morris & Neale, 1954; Businger, 1963), and since then numerous authors have striven to analyse and understand the natural ventilation of greenhouses. Several methods have been used to this end: scale models, tracer gas method, CFD (computational fluids dynamics) simulations and direct measurements in the greenhouse using a variety of sensors. Many of the studies on natural ventilation have employed the tracer gas method, which allows the ventilation rate to be quantified accurately, but provides no information on the airflow characteristics inside the greenhouse (Boulard *et al.*, 1996). Van Buggenhout *et al.* (2009) established that the position of the sensors that detect the concentration of gas can lead to errors of upto 86% and this is particularly relevant if this method is used to validate CFD simulations. The first work to study the natural ventilation of greenhouses using CFD was by Okushima *et al.* (1989). The realism of simulations has improved considerably thanks to the drastically increased capacity of software to process data (Norton *et al.*, 2007). Programmes of CFD have been used to study the microclimate in

---

Abbreviations used. **Nomenclature:**  $C_d$  (total discharge coefficient of the opening);  $C_w$  (wind effect coefficient for the mean airflow); *CFD*, computational fluids dynamics; *RH* (relative humidity [%]); *l* (two-dimensional horizontal resultant of air velocity in XY plane [ $\text{m s}^{-1}$ ]); *q* (specific humidity [ $\text{g g}^{-1}$ ]); *R* (solar radiation [ $\text{W m}^{-2}$ ]);  $S_A$  (greenhouse area [ $\text{m}^2$ ]);  $S_V$  (vent surface area [ $\text{m}^2$ ]); *T* (temperature [ $^{\circ}\text{C}$ ]); *u* (air velocity [ $\text{m s}^{-1}$ ]); *v* (two-dimensional vertical resultant of air velocity in XZ plane [ $\text{m s}^{-1}$ ]). **Greek letters:**  $\Delta$  (difference);  $\Delta T_v$  (vertical temperature gradient [ $^{\circ}\text{C m}^{-1}$ ]);  $\theta$  (wind direction [ $^{\circ}$ ]);  $\sigma$  (standard deviation). Subscripts: *x* (longitudinal component); *y* (transversal component); *z* (vertical component); *s* (sonic); *sc* (sonic corrected); *j* (measurement point); *i* (inside vent surface); *o* (outside); *e* (exterior vent surface). **Superscripts:** *c* (corrected); *n* (normalized).

closed greenhouses (Boulard *et al.*, 1997) and in naturally ventilated ones (Kacira, 1996; Mistriotis *et al.*, 1997; Boulard *et al.*, 1999; Molina-Aiz *et al.*, 2010). These CFD based simulation models require validation by experimental data obtained in the greenhouse, and sonic anemometry is an ideal tool for this purpose.

The present work describes a methodology for studying the natural ventilation of Mediterranean greenhouses using sonic anemometry. Specific programmes have also been designed to facilitate the processing and analysis of the experimental data recorded. This method allows us to study the direction of the airflow at all the greenhouse vents, determining where the air enters and leaves the greenhouse, and therefore to establish the airflow pattern for the greenhouse under conditions of natural ventilation. Their knowledge allows us to improve the current control algorithms that manage the movement of the vents.

## Material and methods

### Experimental setup

The experimental work took place in the western half (24 m × 20 m) of a 1080 m<sup>2</sup> three-span greenhouse located at the agricultural research farm belonging to the University of Almería (36°51' N, 2°16' W). The greenhouse was divided into two halves, as this allows us to study the natural ventilation of each half separately (Fig. 1).

The experiments were carried out with the two side vents (1.05 m × 17.5 m) and the roof vent of the central span (0.97 m × 17.5 m) open. The ventilation surface  $S_V$  represented 11.2% of the of the total greenhouse surface area  $S_A$ . In order to prevent insects entering the greenhouse, insect-proof screens of 13 × 30 threads cm<sup>-2</sup> (0.39 porosity, 164.6 μm pore width, 593.3 μm pore height and 165.5 μm thread diameter) were placed on the vents (Valera *et al.*, 2006). The greenhouse contained a tomato crop (*Solanum lycopersicum* L. cv. Salomee) with an average height of approximately 2.18 m for the first measurement test on 14/05/2009 and 1.90 m for the last one on 18/06/2009, and a leaf area index (m<sup>2</sup> leaf m<sup>-2</sup> ground) of about 2.03 for the first test and 3.09 for the last one.

### Experimental design 1: airflow inside a naturally ventilated greenhouse

To measure the air velocity inside the greenhouse two devices were used, each with three anemometers [Suppl. Fig. 1a (pdf)]. These were placed at 55 different points, making a total of 165 measurement points (Fig. 2). The air velocity was measured over 3 min at each point. This time period is a compromise between a shorter one that may reduce accuracy and a longer one that may increase the overall difference with regard to outside microclimate parameters (Molina-Aiz *et al.*, 2009). As it proved difficult to place the anemometers at the roof vent [Suppl. Fig. 1b (pdf)], this vent was

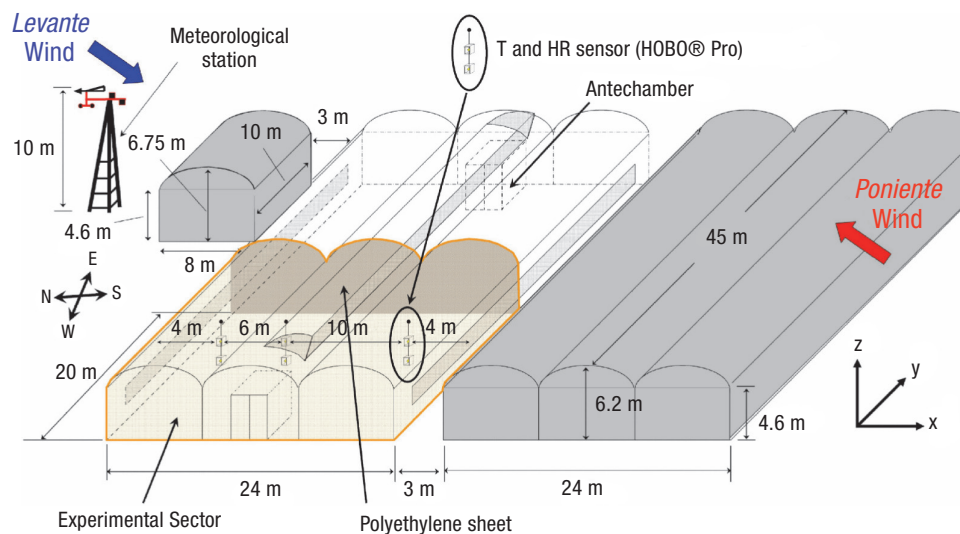


**Figure 1.** Dimensions and location of the experimental greenhouse at the farm.

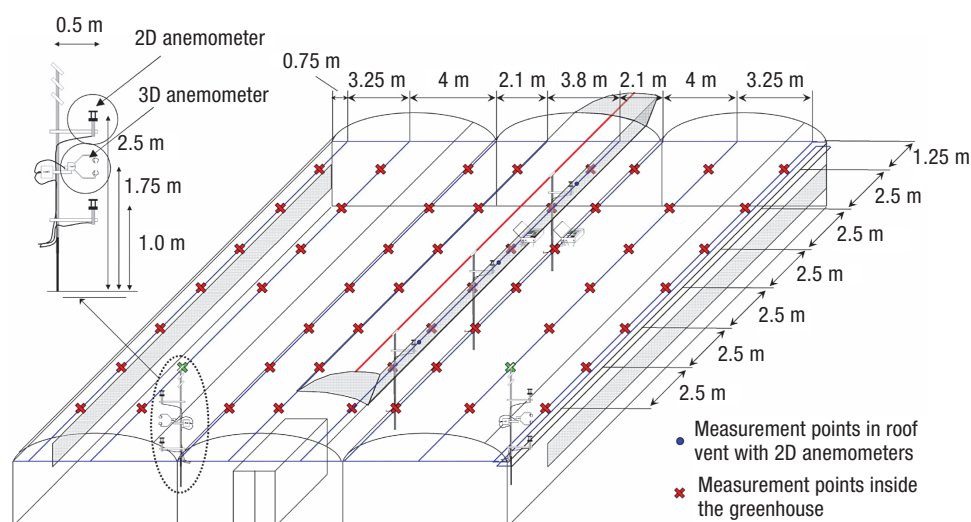


**Figure 2.** Position of measurement points for experimental design 1: airflow inside a naturally ventilated greenhouse.

divided into three equal surfaces and the air velocity measurements were taken continuously at the centre of each surface by three 2D sonic anemometers (Fig. 2).

#### *Experimental design 2: airflow through the side openings*

Simultaneous air velocity measurements were taken at the inside and outside surfaces of the northern side vent in the western sector of the greenhouse (Fig. 3a). These measurements were taken by four pairs of 2D anemometers and one pair of 3D anemometers (Fig. 3a). The anemometers of each pair were located one on the inside and one on the outside [Suppl. Fig. 1c (pdf)], separated by the insect-proof screen. In these experiments all the anemometers were fixed in place and the air velocity was recorded over 30 min. The 3D anemometers were placed at the centre of the vent, and the different pairs of anemometers were placed 3.5 m apart.

#### *Experimental design 3: outside-inside airflow*

For this experiment all the sonic anemometers were placed along a line running perpendicular to the mid-point of the side walls of the western sector (Fig. 3b). Inside the greenhouse, a 3D anemometer was placed at the northern side vent, and five 2D anemometers were placed along the same line running through the inside (Fig. 3b). To measure the outside air velocity four 2D

anemometers and one 3D device were used. These were first placed to the north of the greenhouse (Fig. 3b) and measurements were taken over two 15-min periods (one with the 2D anemometers in a vertical position, measuring the air velocity on the horizontal plane  $XY$ ; and one with them in a horizontal position, measuring the air velocity on the vertical plane  $XZ$ ). Subsequently, they were placed to the south of the greenhouse (Fig. 3b), and again measurements were taken over two 15-min periods.

### **Equipment and instrumentation**

The three components of air velocity and temperature were measured with two 3D sonic anemometers (mod. CSAT3, Campbell Scientific Spain S.L., Spain; resolution:  $0.001 \text{ m s}^{-1}$  and  $0.002^\circ\text{C}$ ; accuracy  $\pm 0.04 \text{ m s}^{-1}$  and  $\pm 0.026^\circ\text{C}$ ). Nine 2D sonic anemometers were also used (mod. Windsonic, Gill Instrument LTD, Lymington, Hampshire, UK; resolution:  $0.01 \text{ m s}^{-1}$ ; accuracy 2%). Data from all sonic anemometers were recorded by two CR3000 Microloggers (Campbell Scientific Spain S.L., Barcelona), with a data registration frequency of 10 Hz (Shilo *et al.*, 2004) for the 3D and 1 Hz (López *et al.*, 2011) for the 2D sonic anemometers.

Outside climatic conditions were recorded by a meteorological station at a height of 10 m located to the north of the greenhouse (Fig. 1). The meteorological station included a BUTRON II (Hortimax S.L.,



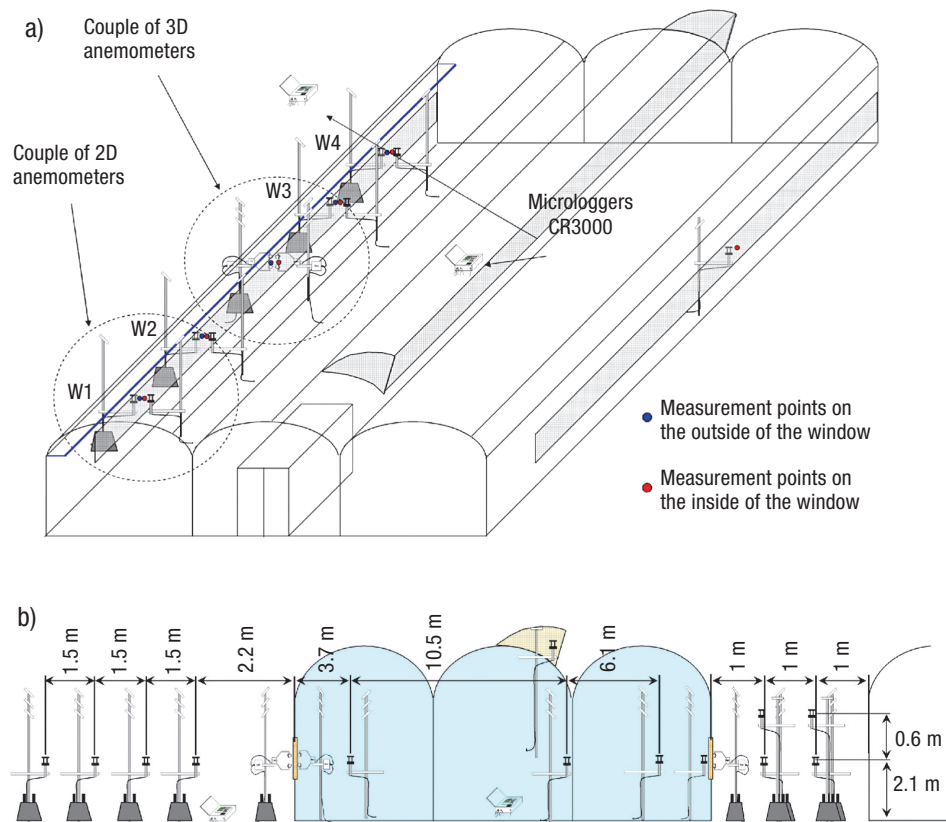


**Figure 3.** Position of measurement points for experimental design 2: airflow through the side openings (a) and for experimental design 3: outside-inside airflow (b).

Almería, Spain) measurement equipped with a temperature sensor Pt1000 IEC 751 class B (Vaisala Oyj, Helsinki, Finland) with a measurement range of  $-10$  to  $60^{\circ}\text{C}$  and an accuracy of  $\pm 0.6^{\circ}\text{C}$ . This box was also equipped with capacitive humidity sensor HUMICAP 180R (Vaisala Oyj) with a measurement range of  $0\%$  to  $100\%$  and accuracy of  $\pm 3\%$ . Outside wind speed was measured with a Meteostation II (Hortimax S.L.), incorporating a cup anemometer with a measurement range of  $0$  to  $40\text{ m s}^{-1}$ , accuracy of  $\pm 5\%$ , and resolution of  $0.01\text{ m s}^{-1}$ . Wind direction was measured with a vane (accuracy  $\pm 5^{\circ}$  and resolution  $1^{\circ}$ ). Solar radiation was measured using a pyranometer sensor Kipp Solari (Hortimax S.L.), with a measurement range of  $0$  to  $2000\text{ W m}^{-2}$ , accuracy of  $\pm 20\text{ W m}^{-2}$ , and resolution of  $1\text{ W m}^{-2}$ .

Temperature and humidity inside the greenhouse were measured using six autonomous data loggers (HOBO Pro Temp-HR U23-001, Onset Computer Corp., Bourne, MA, USA). The data loggers were placed in a vertical profile under the ridge of the three

greenhouse spans at heights of  $1$  and  $2\text{ m}$  (Fig. 1). These fixed devices measure a temperature range of  $-40^{\circ}\text{C}$  to  $70^{\circ}\text{C}$  with an accuracy of  $\pm 0.18^{\circ}\text{C}$  and relative humidity of  $0\%$  to  $100\%$  with an accuracy of  $\pm 2.5\%$ . They were all programmed to register data at  $0.5\text{ Hz}$  and were protected against direct solar radiation with a passive solar radiation open shield. From the data of inside humidity recorded by the fixed sensors, we can obtain the specific humidity  $q$  and correct the sonic anemometer temperature  $T_s$  [ $^{\circ}\text{C}$ ] using the following expression (Tanny *et al.*, 2008):

$$T_{sc} = \frac{T_s}{(1 + 0.51q)} \quad [1]$$

The measurements were done under prevailing *Levante* (northeast) and *Poniente* (southwest) winds, the most usual winds in the province of Almería (Molina-Aiz *et al.*, 2009). The outside climatic conditions remained relatively stable over the six measurement tests (Table 1).

**Table 1.** Outside climatic conditions for the measurement tests. Average wind speed  $u_o$  [ $\text{m s}^{-1}$ ], wind direction  $\theta$  [ $^\circ$ ], outside and inside temperature  $T_o$  and  $T_i$  [ $^\circ\text{C}$ ], outside and inside humidity  $RH_o$  and  $RH_i$  (%) and outside radiation  $R$  [ $\text{W m}^{-2}$ ]

Test – Date	Time	$u_o$	$\theta^1$	$RH_o$	$RH_i$	$T_o$	$T_i$	$R$
<i>Airflow inside the naturally ventilated greenhouse</i>								
1 - 14/05/2009	10:42-12:51	$3.97 \pm 0.80$	$289 \pm 20$	$59 \pm 4$	$69 \pm 2$	$20.5 \pm 0.5$	$24.1 \pm 1.4$	$637 \pm 118$
2 - 15/05/2009	10:37-13:01	$3.55 \pm 1.26$	$183 \pm 15$	$51 \pm 6$	$68 \pm 3$	$22.0 \pm 0.7$	$26.6 \pm 1.0$	$771 \pm 91$
3 - 20/05/2009	10:45-13:05	$3.94 \pm 0.95$	$118 \pm 9$	$37 \pm 2$	$65 \pm 2$	$26.9 \pm 1.0$	$27.4 \pm 1.3$	$732 \pm 125$
4 - 28/05/2009	09:40-11:56	$10.71 \pm 1.11$	$68 \pm 6$	$33 \pm 5$	$51 \pm 5$	$23.2 \pm 0.7$	$23.0 \pm 0.9$	$588 \pm 124$
<i>Airflow through the side openings</i>								
5 - 12/06/2009	10:25-10:55	$10.28 \pm 0.37$	$75 \pm 3$	$19 \pm 1$	$50 \pm 1$	$29.7 \pm 0.5$	$26.0 \pm 0.4$	$539 \pm 28$
6 - 15/06/2009	11:00-11:30	$3.20 \pm 0.28$	$98 \pm 14$	$32 \pm 1$	$72 \pm 2$	$32.0 \pm 0.4$	$28.6 \pm 0.6$	$578 \pm 58$
7 - 17/06/2009	10:58-11:28	$5.77 \pm 0.55$	$96 \pm 7$	$62 \pm 1$	$77 \pm 1$	$26.6 \pm 0.3$	$26.8 \pm 0.3$	$486 \pm 57$
8 - 18/06/2009	10:20-10:50	$5.59 \pm 0.56$	$76 \pm 5$	$64 \pm 1$	$78 \pm 2$	$25.8 \pm 0.1$	$25.4 \pm 0.1$	$295 \pm 10$
<i>Outside-inside airflow</i>								
9 - 12/06/2009	11:20-13:02	$9.23 \pm 0.69$	$74 \pm 5$	$16 \pm 1$	$49 \pm 2$	$31.9 \pm 0.4$	$27.9 \pm 0.5$	$774 \pm 65$
10 - 13/06/2009	11:10-12:52	$2.98 \pm 0.74$	$259 \pm 12$	$38 \pm 2$	$64 \pm 3$	$25.8 \pm 0.5$	$26.6 \pm 0.3$	$711 \pm 53$
11 - 15/06/2009	12:24-14:09	$3.72 \pm 0.40$	$261 \pm 7$	$42 \pm 3$	$64 \pm 2$	$29.9 \pm 0.6$	$31.0 \pm 0.3$	$303 \pm 15$
12 - 17/06/2009	11:49-13:35	$4.40 \pm 0.66$	$92 \pm 13$	$57 \pm 2$	$72 \pm 2$	$27.9 \pm 0.4$	$28.7 \pm 0.7$	$743 \pm 76$

<sup>1</sup> Direction perpendicular to the windows is  $208^\circ$  for a *Poniente* from southwest wind and  $28^\circ$  for a *Levante* from northeast wind.

## Results and discussion

### Description of airflow inside the naturally ventilated greenhouse

#### *Airflow inside the greenhouse with Poniente southwest winds*

Under these conditions the roof vent is facing windward and the windward side vent is blocked by another greenhouse, while the leeward side vent is completely free of obstacles (Fig. 1). Due to the wind effect, air enters the greenhouse through the roof vent and leaves through both side vents, while the thermal effect acts against this, causing the warm air to rise due to buoyancy (see plane XZ in Fig. 4). The counter play of wind and buoyancy effects in the natural ventilation of buildings has been studied in greater depth by Li & Delsante (2001). The air velocity was greater and the direction was more uniform in the southern sector of the greenhouse, which means that the temperature was lower than in the northern sector.

When the air enters through the roof vent it moves northeast, maintaining the same direction as the wind and encountering the central division of the greenhouse, which forces it to change direction and move contrary to the wind direction. The air moves towards the southern side vent to exit the greenhouse and towards the western side, where there is no outlet. Counterflows

inside the greenhouse have been observed by other authors (Wang & Deltour, 1999; Molina-Aiz *et al.*, 2009). Opening the western side of the greenhouse might achieve a better combination of the wind and thermal effects in natural ventilation of the greenhouse.

#### *Airflow inside the greenhouse with Levante northeast winds*

Under prevailing *Levante* winds the roof vent is facing leeward, the windward side vent is free of obstacles and the leeward side vent is blocked by another greenhouse. The air enters through the windward side vent due to the wind effect, rising and leaving through the roof vent. In these circumstances the wind and thermal effects work together. Contrary to what might be expected, air enters through the leeward side vent as it is protected by the other greenhouse structure (Fig. 5).

As air enters through the windward side vent in the northern sector of the greenhouse the wind effect appears to prevail and air does not rise due to buoyancy. However, in the southern sector, the closer to the leeward side vent, the more air is seen to rise due to the thermal effect (see Plane XZ in Fig. 6). Opening the central roof vent alone does not prove to be the most suitable alternative, as the air that rises does not find an exit. The results obtained indicate that opening the roof vent in the southern span of the greenhouse

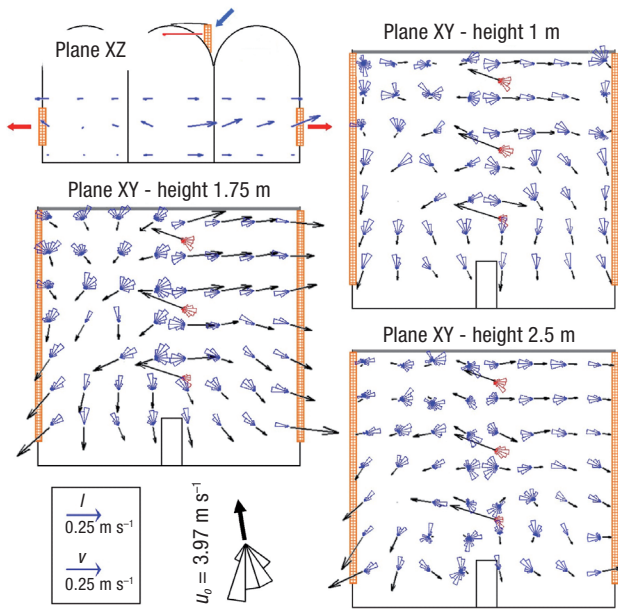


**Figure 4.** Airflow inside the greenhouse. Experiment 1 with prevailing *Poniente* southwest wind. Histograms in blue represent the airflow inside the greenhouse, while those in red represent the airflow at the roof vent ( $l$  and  $v$ , two-dimensional horizontal resultant of air velocity in  $XY$  and  $XZ$  plane, respectively;  $u_o$ , average wind speed).

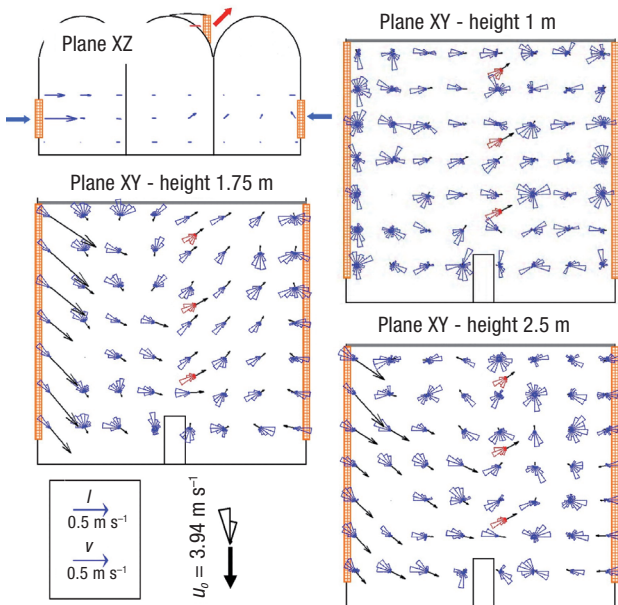


**Figure 5.** Airflow inside the greenhouse. Experiment 3 with prevailing *Levante* wind. Histograms in blue represent the airflow inside the greenhouse, while those in red represent the airflow at the roof vent ( $l$  and  $v$ , two-dimensional horizontal resultant of air velocity in  $XY$  and  $XZ$  plane, respectively;  $u_o$ , average wind speed).

would achieve a better combination of the wind and buoyancy (thermal) effects to foment natural ventilation of the greenhouse.

*Temperature distribution and microclimate inside the greenhouse*

To study the difference in air temperature  $\Delta T_{io}$  from the measurements taken by the 3D sonic anemometers inside the greenhouse, one must bear in mind the variation in climatic conditions inside and outside the greenhouse during the experiments. In a first attempt, the normalised difference in air temperature  $\Delta T_{io}^n$  (Boulard *et al.*, 2000; Kittas *et al.*, 2008) was used:

$$\Delta T_{io}^n = \frac{T_{sc,j} - T_{o,j}}{T_{i,j} - T_{o,j}} \quad [2]$$

where  $T_{sc-j}$  is the corrected sonic temperature (Eq. [1]) obtained for point  $j$ ,  $T_{o,j}$  and  $T_{i,j}$  are the outside and inside air temperatures recorded at measurement point  $j$ . This method of temperature normalisation proved problematic at times when the inside and outside temperatures were very similar, making the denominator in Eq. [2] close to 0. Given this difficulty, the corrected difference in air temperature  $\Delta T_{io}^c$  [°C] was used:

$$\Delta T_{io-j}^c(1) = T_{sc-j}(t) \frac{T_o + T_i}{T_{o-j}(t) + T_{i-j}(t)} - T_o \quad [3]$$

where  $T_o$  and  $T_i$  are the mean outside and inside air temperatures during the experiment (Table 1). Using this method the greenhouse temperature distribution maps were obtained (Fig. 6).

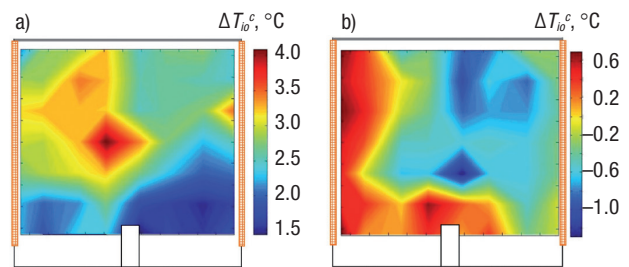


**Figure 6.** Corrected difference in air temperature  $\Delta T_{io}^c$  [°C] inside the greenhouse at a height of 1.75 m. Experiment 1 with prevailing *Poniente* wind (a) and experiment 4 with prevailing *Levante* wind (b).

The heterogeneity of the temperature, the temperature gradient ( $\Delta T_{io}^c$ ) and normalized two-dimensional resultant of air velocity in XZ and XY plane ( $l^n$  and  $v^n$ ) inside the greenhouse was studied by dividing the standard deviation ( $\sigma$ ) of each parameter by its mean (Kittas *et al.*, 2008), and the greater this ratio is, then more heterogeneous is the parameter (Table 2). During the experiment there were variations wind speed and direction, in order to calculate the heterogeneity of the two-dimensional resultant of air velocity in XZ and XY plane ( $l^n$  and  $v^n$ ) we calculated the normalized two-dimensional resultants at each measurement point  $j$  as (Boulard *et al.*, 2000):

$$v_j^n = \frac{v_j(t)}{u_o(t)} \cdot 100 \quad \text{and} \quad l_j^n = \frac{l_j(t)}{u_o(t)} \cdot 100 \quad [4]$$

where  $v_j(t)$  and  $l_j(t)$  are the two-dimensional resultant of air velocity in XZ and XY plane, respectively, measured for the time interval corresponding to point  $j$ , and  $u_o(t)$  is the average wind speed over the same time interval. Greater homogeneity of the temperature inside the greenhouse does not imply a lower gradient between inside and outside temperatures. Kittas *et al.* (2008) studied the microclimate in a single-tunnel greenhouse with different combinations of vents, and they found that the combination that gave rise to the lowest temperature differences between inside and outside was also the one that produced the most heterogeneous temperature distribution. In the experiment carried out on 15/05/2009 (Fig. 6a) under prevailing *Poniente* wind, the air temperature was more uniform than in the one on 28/05/2011 under prevailing *Levante* wind (Fig. 6b). In fact, the most uniform air temperatures were observed in those experiments with the least temperature difference between inside and outside the greenhouse.

A lower vertical temperature gradient was also observed in the experiments carried out under prevailing *Levante* wind, most likely due to the greater heterogeneity of the normalized two-dimensional vertical resultant of air velocity in XZ plane  $v^n$  (Table 2).

Temperature maps (Fig. 6) illustrate at a glance the areas of the greenhouse where most heat accumulates. Under prevailing *Poniente* wind (Fig. 6a) a lot of heat is seen to accumulate in the central part of the greenhouse, as warm air rises due to buoyancy but cannot leave the greenhouse as it encounters a contrary flux due to the wind effect. Under conditions of prevailing *Levante* wind (Fig. 6b), the southern sector of the greenhouse is colder than the outside air, possibly due to the cooling effect of crop evapotranspiration. The greenhouse antechamber constitutes an obstacle to ventilation, causing higher temperatures in the area close to it.

### Description of airflow through the side openings: airflow at the northern side vent, before and after passing through the insect-proof screen

The four experiments for this section were carried out under prevailing *Levante* wind, and so the northern side vent was facing windward. On the horizontal XY plane the airflow outside was almost parallel to the vent surface, and on passing through the insect-proof screen it changed direction. On the vertical XZ plane, the airflow at the outside vent surface had a considerable negative vertical component  $u_z$  which diminished once the air passed through the screen due to the laminating effect of this porous material [Suppl. Fig. 2 (pdf)]. When the side vent was facing windward it was observed that part of the air that approaches the vent

**Table 2.** Vertical temperature gradients  $\Delta T_v$  ( $^{\circ}\text{C m}^{-1}$ ), heterogeneity of the corrected difference in air temperature  $\Delta T_{io}^c$ , of the normalised air velocity on the XY plane ( $l^n$ ) and on the XZ plane ( $v^n$ )

Test	$\Delta T_v$	$\frac{\sigma_{\Delta T_{io}^c}}{\Delta T_{io}^c}$		$\frac{\sigma_{l^n}}{l^n}$		$\frac{\sigma_{v^n}}{v^n}$
		1.75 m	1 m	1.75 m	2.5 m	1.75 m
1	1.2	0.23	0.49	0.47	0.56	0.70
2	2.0	0.35	0.62	0.58	0.78	0.65
3	1.2	1.24	0.56	1.07	1.04	0.96
4	0.4	3.26	1.21	1.62	0.88	1.42



surface does not enter, but rather descends the side of the greenhouse and moves westward.

The air velocity  $u$  is much higher at the outside surface of the vent, falling by 60-85% on entering the greenhouse and passing through the insect-proof screen, but the three orthogonal components are affected differently (Table 3). Much of the airflow that approaches the side vents is diverted sideways or vertically and does not enter the greenhouse. Indeed, the absolute air velocity  $u$  falls by an average 72% on passing through the insect-proof screen into the greenhouse. Due to the diversion of the flow, the transversal  $u_y$  and vertical  $u_z$  components fall by an average 76% and 89%, respectively.

In two of the experiments the longitudinal component,  $u_x$ , perpendicular to the side vent was 3% (experiment 1) and 60% (experiment 2a) less inside than outside, while in the other two experiments this component was higher than outside, increasing by 22% (experiment 3) and 19% (experiment 4). The variations observed in the longitudinal component  $u_x$ , perpendicular to the side vent, are mainly due to the distance of the anemometers from the vent rather than to the effect of the screen. If we were to measure the longitudinal component  $u_x$  just before and after passing through the screen, the air velocity should be the same. The screen would act as a filter, reducing the magnitude of the fluctuations but maintaining their mean value [Suppl. Fig. 3 (pdf)]. The passage of air through porous media such as this causes a laminating effect on the airflow (Fang, 1997). The different behaviour of the three components of air velocity may be due to the orientation of the screen's pores and the layout of the threads. The reduction of the air flux (that enters the greenhouse) due to the insect-proof

screen arises mainly because it prevents the entrance of those air currents that do not flow perpendicular to the pore.

### Description of airflow outside and inside the greenhouse

Fig. 7 represents the airflow outside and in the central span of the western sector of the experimental greenhouse. The barrier to the southern side of the greenhouse may well mean that, whatever the wind direction, the airflow on this side is practically parallel to the side of the greenhouse, making it more difficult for air to enter through the southern side vent.

To determine the reduction in the velocity of the outside air in the proximity of the side vents due to the obstacles, the air velocity measured on the outside was normalised using the mean air velocity recorded by the meteorological station, this values are shown in the Suppl. Table 1 (pdf). In all experiments the normalised air velocity is much lower on the southern side (with obstacles) than on the northern side (without obstacles). If we compare the values recorded on both sides when they are facing windward, under prevailing *Levante* on the northern side the mean value of  $u/u_o$  is 0.769,  $u_x/u_{x,o}$  is 0.234 and  $u_y/u_{y,o}$  is 0.845, while under prevailing *Poniente* on the southern side the value of  $u/u_o$  is 0.017,  $u_x/u_{x,o}$  is 0.029 and  $u_y/u_{y,o}$  is 0.312. In other words, the obstacle on the southern side of the greenhouse causes a mean reduction in air velocity close to the greenhouse when this side is facing windward of 98% for  $u$ , 63% for  $u_y$ , and more strikingly 88% for  $u_x$ , the component of air velocity perpendicular to the side vent.

**Table 3.** Mean values of the air velocity  $u$  [ $\text{m s}^{-1}$ ] and its three orthogonal components  $u_x$ ,  $u_y$  and  $u_z$  [ $\text{m s}^{-1}$ ], before and after passing through the insect-proof screen, measured by 3D sonic anemometry. Subscripts:  $i$ , inside surface;  $o$ , outside surface

Test	Surface	$u$	$u_i/u_o$	$u_x$	$u_{x,i}/u_{x,o}$	$u_y$	$u_{y,i}/u_{y,o}$	$u_z$	$u_{z,i}/u_{z,o}$
5	Inside	$1.94 \pm 1.13$	0.40	$1.12 \pm 0.75^*$	0.97	$-1.56 \pm 1.09$	0.36	$-0.27 \pm 0.32$	0.13
	Outside	$4.89 \pm 2.42$		$1.16 \pm 1.03^*$		$-4.23 \pm 2.71$		$-2.10 \pm 1.58$	
6	Inside	$0.16 \pm 0.10$	0.15	$0.04 \pm 0.14^*$	0.40	$-0.11 \pm 0.08$	0.11	$0.07 \pm 0.04$	0.25
	Outside	$1.09 \pm 0.79$		$0.10 \pm 0.22^*$		$-1.03 \pm 0.85$		$-0.28 \pm 0.44$	
7	Inside	$0.49 \pm 0.39$	0.23	$0.28 \pm 0.40^*$	1.22	$-0.39 \pm 0.34$	0.20	$0.01 \pm 0.11$	0.01
	Outside	$2.15 \pm 1.45$		$0.23 \pm 0.50^*$		$-2.00 \pm 1.53$		$-0.72 \pm 0.85$	
8	Inside	$1.12 \pm 0.55$	0.34	$0.69 \pm 0.36^*$	1.19	$-0.88 \pm 0.50$	0.29	$-0.04 \pm 0.11$	0.04
	Outside	$3.26 \pm 1.43$		$0.58 \pm 0.47^*$		$-3.01 \pm 1.57$		$-1.09 \pm 0.86$	

\* No statistical difference between inside and outside vent surfaces (95% confidence level; LSD method).

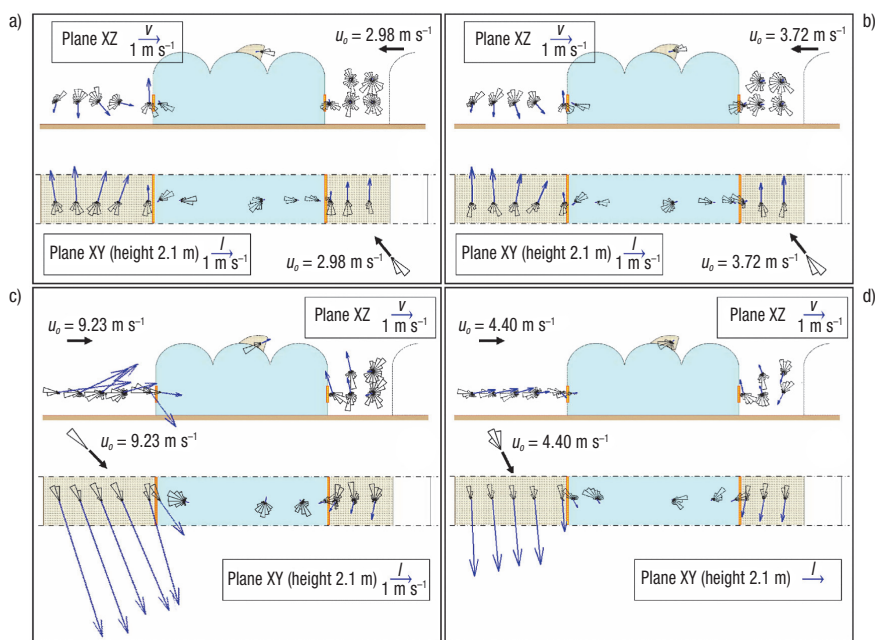


**Figure 7.** Cross-section through the middle of the western sector of the greenhouse representing the airflow. Experiments 10 (a) and 11 (b) under prevailing *Poniente* wind, and experiments 9 (c) and 12 (d) under prevailing *Levante* wind.

### Airflow pattern outside and inside the experimental greenhouse

The results obtained from the different experimental designs allowed us to create a model illustrating how the air moves both outside and inside the greenhouse for both wind directions (Figs. 8a,b). Most noteworthy is the fact that little air flows perpendicular to the side vents, especially on the blocked southern side. This shows the barrier effect of the adjacent greenhouse. When the wind approaches the windward side vent, as it has to overcome an obstacle eddies are formed at the

side of the greenhouse, making it difficult for air to enter. *Poniente* winds must overcome two obstacles before reaching the northern side vent: the neighbouring greenhouse to the south and the experimental greenhouse itself. *Levante* winds have a direct impact on the northern side vent which is free of obstacles. Natural ventilation inside the greenhouse is less effective under prevailing *Poniente* winds, since the air has to enter through the roof vent and runs contrary to the thermal effect. The air exits through the side vents, but when the air among the plants warms up it rises instead of heading towards the vents. When the *Levante* pre-

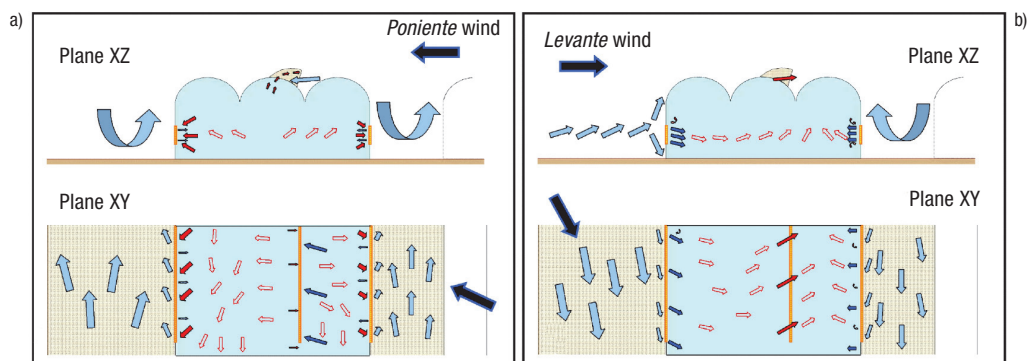


**Figure 8.** Airflow pattern outside the greenhouse and inside the western sector for the two most frequent winds, *Poniente* (a) and *Levante* (b).

vails the air enters through the side vents and leaves through the roof vent, fomenting the exit of warm air that rises due to buoyancy.

Once the airflow pattern has been established for both inside and outside, we are in a position to make a series of proposals that could substantially improve the natural ventilation of the experimental greenhouse. For instance, certain modifications regarding the placing of the side vents can be proposed with a view to improving the entrance of outside air. One option would be to install vents equipped with ailerons which guide the air, or with vents in which the screen is not placed directly over the side surface of the greenhouse (Fig. 9). Another option would be to design an antechamber where the air can enter without encountering the screen, which would be placed further inside the greenhouse. A different proposal is to prolong the opening of the side vents down to the soil, thus fomenting the entrance of air at crop level. Bailey (2003) proposes making several folds in the roof screen of the greenhouse, similar to those of an accordion, in order to increase the surface area of the screen through which the air passes, thus reducing the drawback of using screens of high porosity. This is along similar lines to the idea of using the different designs of the side vents presented in Fig. 9.

The design of natural ventilation in a greenhouse must allow for different vent setups, in such a way that the most suitable degree of opening can be set for each vent, either manually or automatically, depending on the wind direction, with a view to achieving the best possible combination of the wind and thermal effects. It is important that these two effects work in conjunction to foment natural ventilation, rather than counteracting one another as happens in the experimental greenhouse when *Poniente* wind prevails.

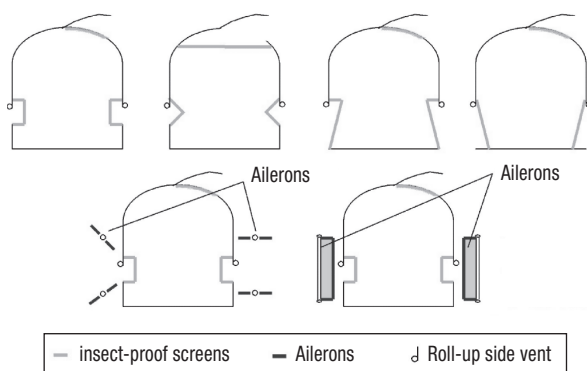


**Figure 9.** Proposals of alternative setups for vents, insect-proof screens and ailerons (outside the greenhouse).

As conclusions, the use of sonic anemometry has allowed us to identify the vents through which air enters and exits the greenhouse, and therefore to establish the airflow patterns caused by natural ventilation. The setup of two side vents and one roof vent has given rise to two quite different situations. The air velocity, the direction of the roof vent (windward or leeward) and the presence of obstacles close to the side vents have a significant bearing on the air flux due to the thermal effect (buoyancy), rising towards the roof vent, and the air flux due to the wind effect. When the roof vent faces leeward, cool air moves through the side vents due to the wind effect, heading towards the roof vent through which it leaves warmer, mixed with the air which moves due to the thermal effect. However, when the roof vent faces windward the outside air passes through it, competing with the air which is rising due to the natural convection of the thermal effect.

The obstacles on the southern side of the experimental greenhouse cause a mean reduction in air velocity close to the greenhouse when facing windward of 98% for  $u$ , 63% for  $u_y$ , and more importantly 88% for  $u_x$ , the component of air velocity that is perpendicular to the side vent.

The methodology followed in the present work has allowed us to obtain patterns of natural ventilation of the experimental greenhouse under the most common wind regimes for this region. It has also enabled us to describe how the wind and thermal effects interact in the natural ventilation of the greenhouse, as well as to detect deficiencies in the ventilation of the greenhouse, caused by the barrier effect of the adjacent greenhouse. Several solutions to improve the ventilation of the tested greenhouse are proposed.

## Acknowledgements

This work has been financed by the *Junta de Andalucía* and the *Ministerio de Economía y Competitividad* by means of the research grants P09-AGR-4593 and AGL2010-22284-C03-01, respectively.

## References

- Bailey BJ, 2003. Screens stop insects but slow airflow. *Fruit Veg Technol* 3: 6-8.
- Bot GPA, 1983. Greenhouse climate: From physical processes to a dynamic model. Doctoral thesis. Agr Univ Wageningen, Wageningen, The Netherlands.

- Boulard T, Baille A, 1995. Modelling of air exchange rate in a greenhouse equipped with continuous roof vents. *J Agr Eng Res* 61(1): 37-48.
- Boulard T, Meneses JF, Mermier M, Papadakis G, 1996. The mechanisms involved in the natural ventilation of greenhouses. *Agr Forest Meteorol* 79: 61-77.
- Boulard T, Feuilloley P, Kittas C, 1997. Natural ventilation performance of six greenhouse and tunnel types. *J Agr Eng Res* 67(4): 249-266.
- Boulard T, Haxaire R, Lamrani MA, Roy JC, Jaffrin A, 1999. Characterization and modelling of the air fluxes induced by natural ventilation in a greenhouse. *J Agr Eng Res* 74: 135-144.
- Boulard T, Wang S, Haxaire R, 2000. Mean and turbulent air flows and microclimatic patterns in an empty greenhouse tunnel. *Agr Forest Meteorol* 100: 169-181.
- Bruce JM, 1978. Natural convection through openings and its applications to cattle building ventilation. *J Agr Eng Res* 23(2): 151-167.
- Bruce JM, 1982. Ventilation of a model livestock building by thermal buoyancy. *T ASAE* 25(6): 1724-1726.
- Businger JA, 1963. The glasshouse (greenhouse) climate. In *Physics of plant environment*. Ed. van Wijk, North-Holland Publ. Co., Amsterdam. pp: 277-318.
- Fang F, 1997. A design method for contractions with square end sections. *T ASME* 119: 454-458.
- Fatnassi H, Boulard T, Demrati H, Bouirden L, Sappe G, 2002. Ventilation performance of a large Canarian-type greenhouse equipped with insect-proof nets. *Biosyst Eng* 82(1): 97-105.
- Kacira M, 1996. Modeling dynamic air exchanges for naturally ventilated sawtooth greenhouse designs. Doctoral thesis. Ohio Stat Univ, Wooster, OH, USA.
- Kittas C, Boulard T, Mermier M, Papadakis G, 1996. Wind induced air exchange rates in a greenhouse tunnel with continuous side openings. *J Agr Eng Res* 65(1): 37-49.
- Kittas C, Boulard T, Papadakis G, 1997. Natural ventilation of a greenhouse with ridge and side openings: sensitivity to temperature and wind effects. *T ASAE* 40(2): 415-425.
- Kittas C, Katsoulas N, Bartzanas T, Mermier M, Boulard T, 2008. The impact of insect screens and ventilation openings on the greenhouse microclimate. *T ASABE* 51(6): 2151-2165.
- Li Y, Delsante A, 2001. Natural ventilation induced by combined wind and thermal forces. *Build Environ* 36: 59-71.
- López A, Valera DL, Molina-Aiz FD, 2011. Sonic anemometry to measure natural ventilation in greenhouses. *Sensors* 11: 9820-9838.
- Mistriosis A, Bot GPA, Picuno P, Scarascia-Mugnozza G, 1997. Analysis of the efficiency of greenhouse ventilation using computational fluid dynamics. *Agr Forest Meteorol* 85: 217-228.
- Molina-Aiz FD, Valera DL, Peña AA, Gil JA, López A, 2009. A study of natural ventilation in an Almería-type greenhouse with insect screens by means of tri-sonic anemometry. *Biosyst Eng* 104: 224-242.
- Molina-Aiz FD, Fatnassi H, Boulard T, Roy JC, Valera DL, 2010. Comparison of finite element and finite volume methods for simulation of natural ventilation in greenhouses. *Comput Electr Agr* 72: 69-86.
- Molina-Aiz FD, Valera DL, López A, 2011. Airflow at the openings of a naturally ventilated Almería-type greenhouse with insect-proof screens. *Acta Hort* 893: 545-552.
- Morris LG, Neale FE, 1954. The infra-red carbon dioxide gas analyser and its use in glasshouse research. *Nat Inst Agr Eng. Tech Memo No. 99*, Silsoe, UK, 13 pp.
- Norton T, Sun D, Grant J, Fallon R, Dodd V, 2007. Applications of computational fluid dynamics (CFD) in the modelling and design of ventilation systems in the agricultural industry: a review. *Bioresour Technol* 98: 2386-2414.
- Okushima L, Sase S, Nara M, 1989. A support system for natural ventilation design of greenhouses based on computational aerodynamics. *Acta Hort* 284: 129-136.
- Papadakis G, Mermier M, Meneses JF, Boulard T, 1996. Measurement and analysis of air exchange rates in a greenhouse with continuous roof and side openings. *J Agr Eng Res* 63: 219-228.
- Sase S, Takakura T, Nara M, 1984. Wind tunnel testing on airflow and temperature distribution of a naturally ventilated greenhouse. *Acta Hort* 148: 329-336.
- Shilo E, Teitel M, Mahrer Y, Boulard T, 2004. Air-flow patterns and heat fluxes in roof-ventilated multi-span greenhouse with insect-proof screens. *Agr Forest Meteorol* 122: 3-20.
- Tanny J, Haslavsky V, Teitel M, 2008. Airflow and heat flux through the vertical opening of buoyancy-induced naturally ventilated enclosures. *Energ Building* 40: 637-646.
- Teitel M, Liran O, Tanny J, Barak M, 2008. Wind driven ventilation of a mono-span greenhouse with a rose crop and continuous screened side vents and its effect on flow patterns and microclimate. *Biosyst Eng* 101(1): 111-122.
- Valera DL, Álvarez AJ, Molina FD, 2006. Aerodynamic analysis of several insect-proof screens used in greenhouses. *Span J Agric Res* 4(4): 273-279.
- Van Buggenhout S, Van Brecht A, Eren Özcan S, Vranken E, Van Malcot W, Berckmans D, 2009. Influence of sampling positions on accuracy of tracer gas measurements in ventilated spaces. *Biosyst Eng* 104: 216-223.
- Wang S, Deltour J, 1999. Lee-side ventilation-induced air movement in a large-scale multi-span greenhouse. *J Agr Eng Res* 74: 103-110.